Supplementary material: Photonic Implementation of Quantum Gravity Simulator

Emanuele Polino, Beatrice Polacchi, Davide Poderini, Iris Agresti, Gonzalo Carvacho, and Fabio Sciarrino
Dipartimento di Fisica, Sapienza Università di Roma, P.le Aldo Moro 5, I-00185 Roma, Italy

Andrea Di Biagio
Dipartimento di Fisica, Sapienza Università di Roma, Piazzale Aldo Moro 5, Roma, Italy and
Institute for Quantum Optics and Quantum Information (IQOQI) Vienna,
Austrian Academy of Sciences, Boltzmanngasse 3, A-1090 Vienna, Austria

Carlo Rovelli
Aix-Marseille University, Université de Toulon, CPT-CNRS, Marseille, France,
Department of Philosophy and the Rotman Institute of Philosophy, Western University, London ON, Canada, and
Perimeter Institute, 31 Caroline Street N, Waterloo ON, Canada

Marios Christodoulou
Institute for Quantum Optics and Quantum Information (IQOQI) Vienna,
Austrian Academy of Sciences, Boltzmanngasse 3, A-1090 Vienna, Austria and
Vienna Center for Quantum Science and Technology (VCQ), Faculty of Physics,
University of Vienna, Boltzmanngasse 5, A-1090 Vienna, Austria

I. DETAILS ON THE PHOTONIC SIMULATOR SCHEME

The implementation of the Quantum Circuit Simulator (Fig. S1a) is realized with the linear optical scheme depicted in Fig. S1b (see Ref.[44]) and implemented by the apparatus in Fig. S1c. We focus now on the linear optical scheme (Fig. S1b). Here, we map the gravitational field basis states $\{|g_{LR}\rangle, |g_{LL}\rangle, |g_{RR}\rangle, |g_{RL}\rangle\}$, introduced in Eq. (1) of the main text, to the path degree of freedom of two single photons, represented by the following basis states $\{|l_1\rangle, |l_2\rangle, |l_3\rangle, |l_4\rangle\}$, where the state $|l_i\rangle$ represents a photon along the path i (with $i = 1, ..., 4$). Their spin basis states $\{|\uparrow\rangle, |\downarrow\rangle\}$, instead, are simulated through the vertical and horizontal photon polarizations $\{|V\rangle, |H\rangle\}$. Exploiting these two degrees of freedom, each step of the logic circuit can straightforwardly be implemented by means of linear optical elements.

The preparation stage (a Hadamard gate for each spin qubit) of the two polarization states gives rise to the product state $(|H\rangle + |V\rangle))/\sqrt{2} \otimes (|H\rangle + |V\rangle))/\sqrt{2}$. Then, the superposition step is realized by two polarizing beam splitters (PBS) that deterministically perform a control-NOT gate, entangling the polarization and path degrees of freedom of each photon (Fig. S1b). The global state, tensor product of two entangled states, reads:

$$|\Psi\rangle = \frac{1}{2}\left[(|H\rangle|l_1\rangle + |V\rangle|l_2\rangle) \otimes (|H\rangle|l_3\rangle + |V\rangle|l_4\rangle)\right] , \tag{1}$$

Then, the path qubits of the two photons, representing the two gravitational fields of the masses, are subject to a control-Phase (CZ) gate, to mimic gravitational interaction of the masses mediated by gravitational field. In order to act only on the path degree of freedom independently of polarization (according to the assumption that the masses do not interact directly), two half-waveplates rotated by 45° are inserted along paths 1 and 3. In this way the state becomes:

$$|\Psi\rangle' = \frac{1}{2}[\,(|l_1\rangle + |l_2\rangle) \otimes (|l_3\rangle + |l_4\rangle)\,|V\rangle\,|V\rangle\,] , \tag{2}$$

so that the polarization and path are factorized. This allows the "gravitational gate" (Free Fall stage in Fig.S1a) to act only on the path degree of freedom.

At this point, it is convenient to switch to the second quantization formalism describing photon number states along the modes through annihilation and creation operators.

In this formalism the state of a photon along a mode $\boldsymbol{k}$, that comprises all photon's degrees of freedom, can be described by the annihilation and creation operators, denoted by $a_{\boldsymbol{k}}$ and $a^\dagger_{\boldsymbol{k}}$, respectively. Such operators obey the following bosonic commutation rules:

$$[a_{\boldsymbol{k_i}}, a_{\boldsymbol{k_j}}] = [a^\dagger_{\boldsymbol{k_i}}, a^\dagger_{\boldsymbol{k_j}}] = 0 \qquad\qquad [a_{\boldsymbol{k_i}}, a^\dagger_{\boldsymbol{k_j}}] = \delta_{ij} , \tag{3}$$

where $\boldsymbol{k_i}$ and $\boldsymbol{k_j}$ are two modes of the field.

Fock states, represented by $|n_{\boldsymbol{k}},\ldots\rangle$, are states with a fixed number $n_{\boldsymbol{k}}$ of photons along each mode. The action of annihilation (creation) operators on such states is to destroy (create) a photon along mode $\boldsymbol{k}$, according to the relations:

$$a_{\boldsymbol{k}}\,|n_{\boldsymbol{k}}\rangle = \sqrt{n_{\boldsymbol{k}}}\,|n_{\boldsymbol{k}}-1\rangle \qquad a^\dagger_{\boldsymbol{k}}\,|n_{\boldsymbol{k}}\rangle = \sqrt{n_{\boldsymbol{k}}+1}\,|n_{\boldsymbol{k}}+1\rangle\ . \tag{4}$$

In particular, one can generate any Fock state from vacuum state $|0\rangle$, by iteratively applying creation operators on the modes: $|n_{\boldsymbol{k}}\rangle = \frac{{a^\dagger_{\boldsymbol{k}}}^{n_{\boldsymbol{k}}}}{\sqrt{n_{\boldsymbol{k}}!}}|0\rangle$.

The unitary evolution U on operators $a^\dagger_i$ can be described by the following relation:

$$a^\dagger_i \to \sum_j U^\dagger_{ij}\, b^\dagger_j\ , \tag{5}$$

where $b^\dagger_j$ represent the output modes of the transformation.

We now describe the scheme [44] which performs the control-Phase in the path degree of freedom of photons in our platform. Since the polarization state factorizes, it is omitted.

Such a scheme is composed of three parallel two-mode couplers, that allow the interference of two input modes. The expression of each coupler is:

$$U_R = \begin{pmatrix} i\sqrt{R} & \sqrt{1-R} \\ \sqrt{1-R} & i\sqrt{R} \end{pmatrix}\ , \tag{6}$$

For instance, consider the upper coupler between modes 1 and $out1$ in Fig. S1b. The mode corresponding to the operator $a^\dagger_1$ can be transmitted with probability amplitude $\sqrt{1-R}$ and reflected with amplitude $i\sqrt{R}$. Therefore it evolves as: $a^\dagger_1 \to \sqrt{1-R}\ b^\dagger_{out1} - i\sqrt{R}\ b^\dagger_1$, where $b^\dagger_1$ and $b^\dagger_{out1}$ represent the transmitted and reflected creation mode operators, respectively. Three parallel couplers $U_{out1\,,1}$, $U_{2\,,3}$, $U_{4\,,out4}$, with $R = 1/3$, allow to interfere the mode pairs $(out1, 1)$, $(2, 3)$ and $(4, out4)$, respectively. Modes $out1$ and $out4$ are vacuum ancillary modes whose utility will be clarified later. Consider all four possible two-photon states in which we have a photon along mode 1 or 2 (first photon) and a photon along mode 3 or 4 (second photon).

Exploiting relation (5) and definition (6), one obtains, for each considered input state, the following transformation under the global evolution $U_{CZ} = U_{out1\,,1} \otimes U_{2\,,3} \otimes U_{4\,,out4}$:

$$\begin{aligned}
&|l_1\rangle\,|l_3\rangle \equiv |1\rangle_1|1\rangle_3 = a^\dagger_1 a^\dagger_3|0\rangle \xrightarrow{U_{CZ}} \\
&\left(\sqrt{\frac{2}{3}}b^\dagger_{out1} - i\frac{1}{\sqrt{3}}b^\dagger_1\right)\left(\sqrt{\frac{2}{3}}b^\dagger_2 - i\frac{1}{\sqrt{3}}b^\dagger_3\right)|0\rangle = \\
&= \frac{2}{3}|1\rangle_{out1}|1\rangle_2 - i\frac{\sqrt{2}}{3}(|1\rangle_{out1}|1\rangle_3 + |1\rangle_1|1\rangle_2) - \frac{1}{3}|1\rangle_1|1\rangle_3\ ,
\end{aligned} \tag{7}$$

$$\begin{aligned}
&|l_1\rangle\,|l_4\rangle \equiv |1\rangle_1|1\rangle_4 = a^\dagger_1 a^\dagger_4|0\rangle \xrightarrow{U_{CZ}} \\
&\left(\sqrt{\frac{2}{3}}b^\dagger_{out1} - i\frac{1}{\sqrt{3}}b^\dagger_1\right)\left(\sqrt{\frac{2}{3}}b^\dagger_{out4} - i\frac{1}{\sqrt{3}}b^\dagger_4\right)|0\rangle = \\
&= \frac{2}{3}|1\rangle_{out1}|1\rangle_{out4} - i\frac{\sqrt{2}}{3}(|1\rangle_{out1}|1\rangle_4 + |1\rangle_1|1\rangle_{out4}) + \\
&- \frac{1}{3}|1\rangle_1|1\rangle_4\ ,
\end{aligned} \tag{8}$$

$$\begin{aligned}
&|l_2\rangle\,|l_3\rangle \equiv |1\rangle_2|1\rangle_3 = a^\dagger_2 a^\dagger_3|0\rangle \xrightarrow{U_{CZ}} \\
&\left(\sqrt{\frac{2}{3}}b^\dagger_3 - i\frac{1}{\sqrt{3}}b^\dagger_2\right)\left(\sqrt{\frac{2}{3}}b^\dagger_2 - i\frac{1}{\sqrt{3}}b^\dagger_3\right)|0\rangle = \\
&= \frac{2}{3}|1\rangle_3|1\rangle_2 - i\frac{2\sqrt{2}}{3}(|2\rangle_3 + |2\rangle_2) - \frac{1}{3}|1\rangle_2|1\rangle_3 = \\
&= \frac{1}{3}|1\rangle_2|1\rangle_3 - i\frac{2\sqrt{2}}{3}(|2\rangle_3 + |2\rangle_2)\ ,
\end{aligned} \tag{9}$$

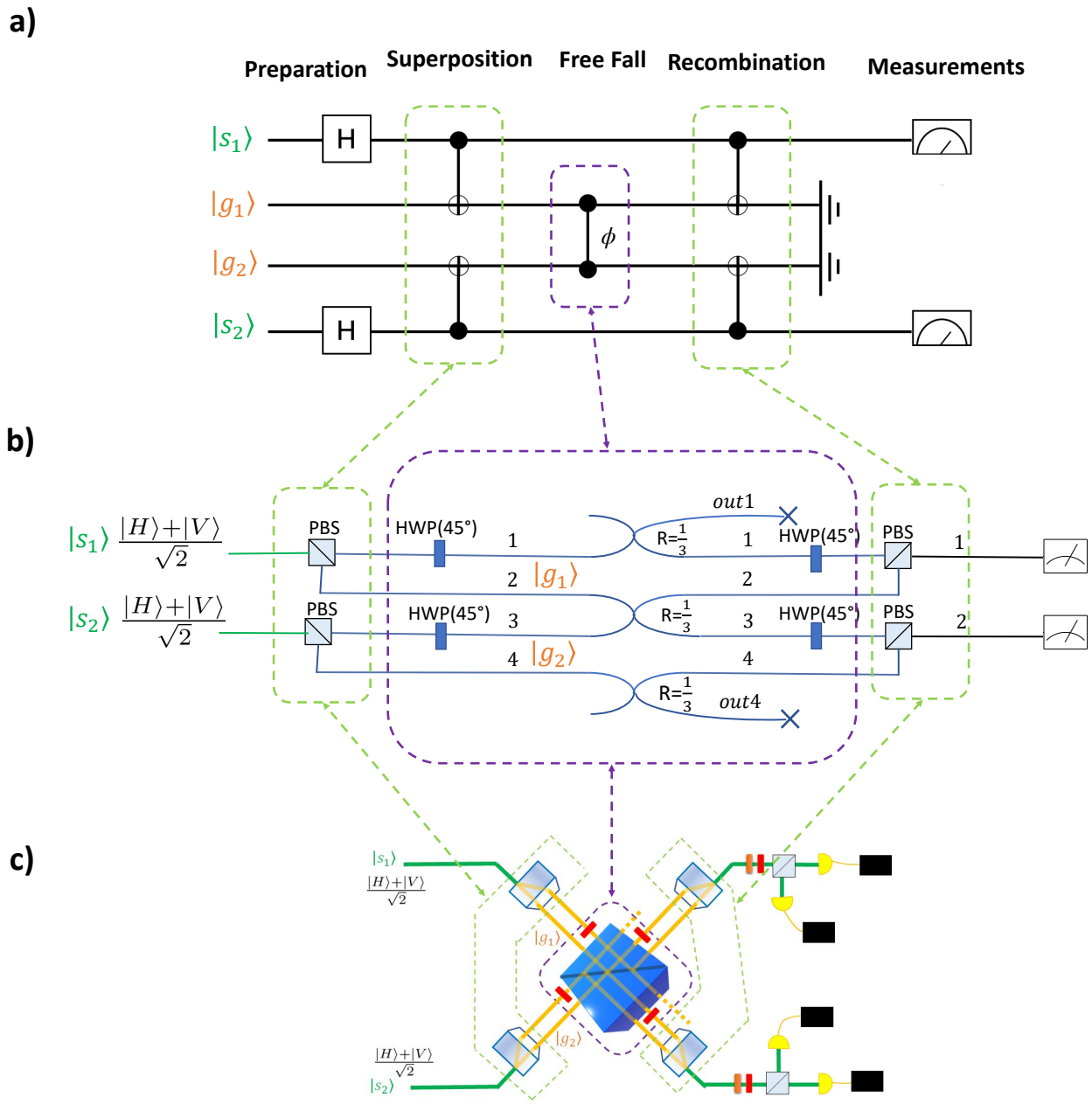

FIG. S1: **Linear optical scheme for Quantum Circuit simulator.** Comparison between **a)** the circuital scheme, **b)** the optical scheme and **c)** the realized implementation of the optical scheme. The spin qubits of the simulator are encoded in the polarization degrees of freedom of the two photons, while the geometry degrees of freedom are encoded in their paths. The CZ gate in the path degree of freedom is implemented using the scheme in [44]. H=Hadamard gate, PBS=polarizing beam splitter, HWP=half-waveplate.

$$
\begin{aligned}
&|l_2\rangle\,|l_4\rangle \equiv |1\rangle_2|1\rangle_4 = a_2^\dagger a_4^\dagger|0\rangle \xrightarrow{U_{CZ}} \\
&\left(\sqrt{\frac{2}{3}}b_3^\dagger - i\frac{1}{\sqrt{2}}b_2^\dagger\right)\left(\sqrt{\frac{2}{3}}b_{out4}^\dagger - i\frac{1}{\sqrt{3}}b_4^\dagger\right)|0\rangle = \\
&= \frac{2}{3}|1\rangle_3|1\rangle_{out4} - i\frac{\sqrt{2}}{3}(|1\rangle_3|1\rangle_4 + |1\rangle_2|1\rangle_{out4}) - \frac{1}{3}|1\rangle_2|1\rangle_4\ ,
\end{aligned}
\tag{10}
$$

where $|n\rangle_x$ indicates the Fock state with n photons along x mode and the last equality of Eq. (9) used the indistinguishability of the photons. Post-selecting the final states where there are one and only one photon along modes 1 or 2, and simultaneously one and only one photon along modes 3 or 4, the above transformations reduce to the following four transformations: $|1\rangle_1 |1\rangle_3 \xrightarrow{U_{CZ}} -|1\rangle_1 |1\rangle_3 /3$, $|1\rangle_1 |1\rangle_4 \xrightarrow{U_{CZ}} -|1\rangle_1 |1\rangle_4 /3$, $|1\rangle_2 |1\rangle_3 \xrightarrow{U_{CZ}} +|1\rangle_2 |1\rangle_3 /3$, $|1\rangle_2 |1\rangle_4 \xrightarrow{U_{CZ}} -|1\rangle_2 |1\rangle_4 /3$. Each term evolves to a post-selected state with probability $1/9$. Hence, multiplying each term to -1 and defining for simplicity the logic states $|0\rangle_T \equiv |l_1\rangle = |1\rangle_1$, $|1\rangle_T \equiv |l_2\rangle = |1\rangle_2$, $|0\rangle_C \equiv |l_4\rangle = |1\rangle_4$, $|1\rangle_C \equiv |l_3\rangle = |1\rangle_3$, the post-selected transformation is:

$$\begin{cases} |0\rangle_T |0\rangle_C & \longrightarrow & |0\rangle_T |0\rangle_C \\ |0\rangle_T |1\rangle_C & \longrightarrow & |0\rangle_T |1\rangle_C \\ |1\rangle_T |0\rangle_C & \longrightarrow & |1\rangle_T |0\rangle_C \\ |1\rangle_T |1\rangle_C & \longrightarrow & -|1\rangle_T |1\rangle_C \end{cases} , \tag{11}$$

that corresponds to a control-Phase operation between the two qubits encoded in the path degree of freedom of the photons.

Such a scheme is implemented by the setup in Fig. S1c where a central beam splitter acts on different modes interfering in three points, while four beam displacers act pairwise to split and recombine the photons based on their polarizations.

We note that the post-selection here is not essential in the actual massive experiments but only plays a role in this particular implementation of the GME simulation.

II. ENTANGLEMENT DEGRADING EFFECTS AND QUANTUM STATE TOMOGRAPHIES

In the experimental simulation, we studied two kinds of noisy effects that could be observed in future massive experiments, preventing the formation or the detection of entanglement.

The first effect studied, as explained in the main text, is the decoherence of the state that could be due to either gravitational induced collapse or to the coupling of the degrees of freedom of the masses with the environment and is one of the major obstacles to a proper realization of massive GME experiments. In Fig. S2, we show the quantum state tomographies of states with different degrees of coherence, i.e. for different parameter values η in Eq. (11) of the main text. Decoherence was induced by using birefringent plates of different widths. Birefringence causes horizontal and vertical polarizations to experience different refraction indices, and they are thus time delayed one with respect to the other, with a time-delay depending on the plate width.

The second effect studied is the temporal indistinguishability of the photon in the degree of freedom of time arrival: if the two photons run across the interferometer at different times, they will not interfere and no entanglement will arise between them. This can simulate the effect of non-synchronized time of the masses, or a screened interaction that would prevent the generation of entanglement. In Fig.S3 we show the quantum state tomographies of states with different degrees of distinguishability $1 - v$ in Eq.(12) of the main text, which is tuned by varying the delay between the two photons before the beam splitter.

Finally, for the different degrees of indistinguishability we also measured the entanglement witness as reported in Fig.S4.

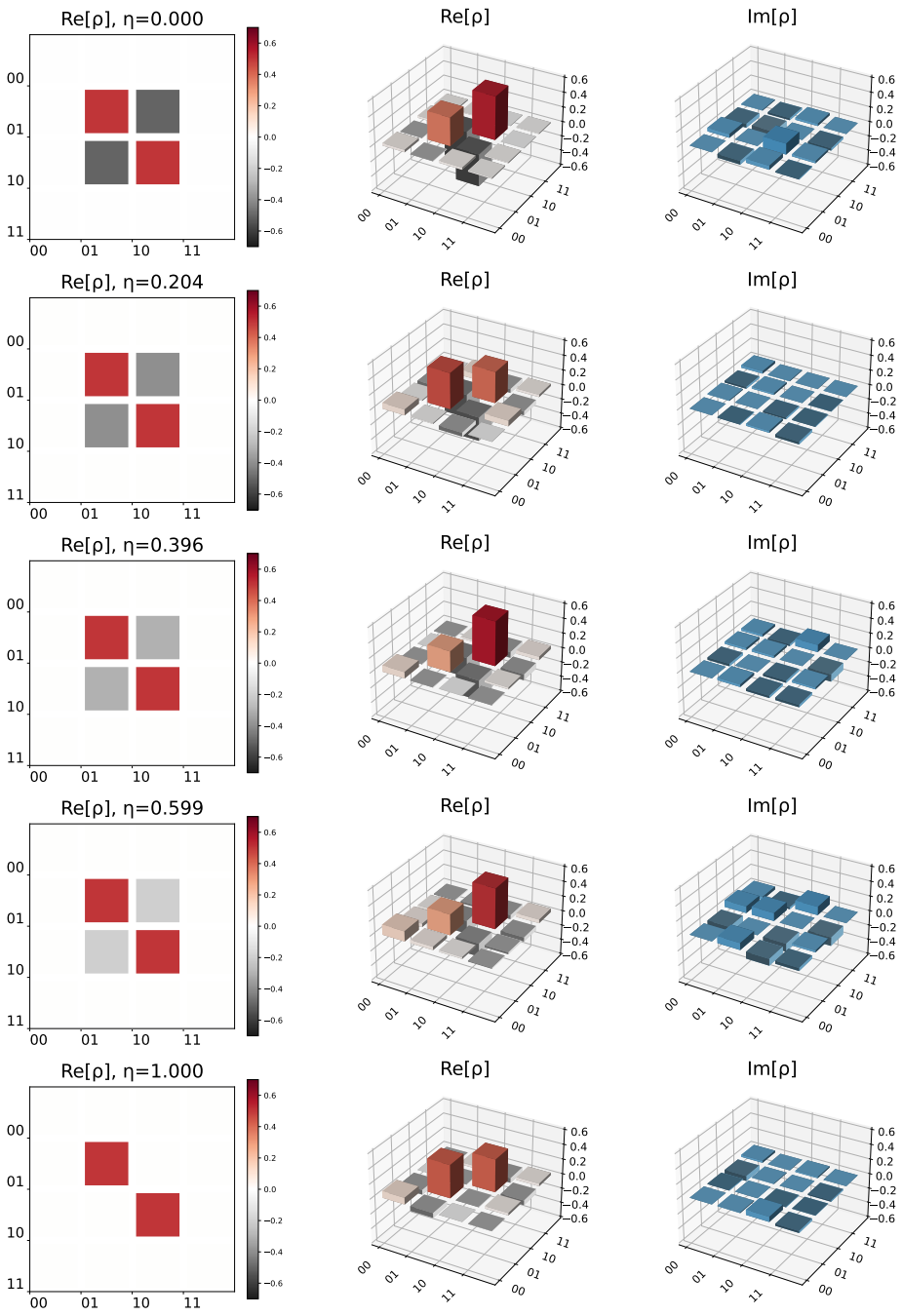

FIG. S2: **Results of QC simulator with decoherence effect.** Experimental real (left) and imaginary (right) parts of the measured density matrices of the polarization states of the spin qubits, generated after the Free Fall stage and post selection of the geometry qubits, as function of the degree of decoherence η in Eq.(11) of the main text.

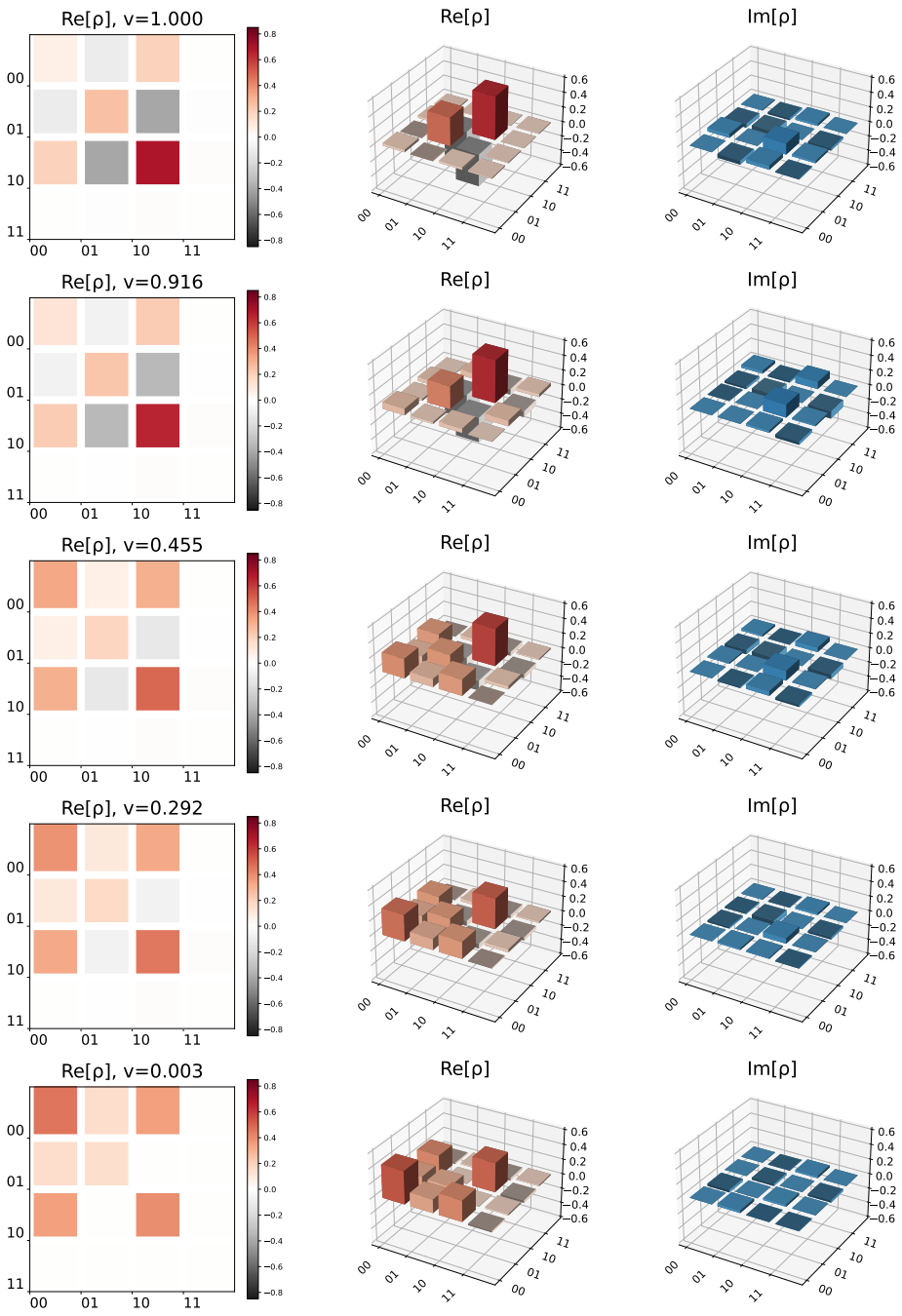

FIG. S3: **Results of QC simulator with varying photon distinguishability.** Experimental real (left) and imaginary (right) parts of the measured density matrices of the polarization states of the spin qubits, generated after the Free Fall stage and post selection of the geometry qubits, at different temporal delays between the two photons. The distinguishability degree $(1 - v)$ extracted from fits on the experimental data is reported above each tomography.

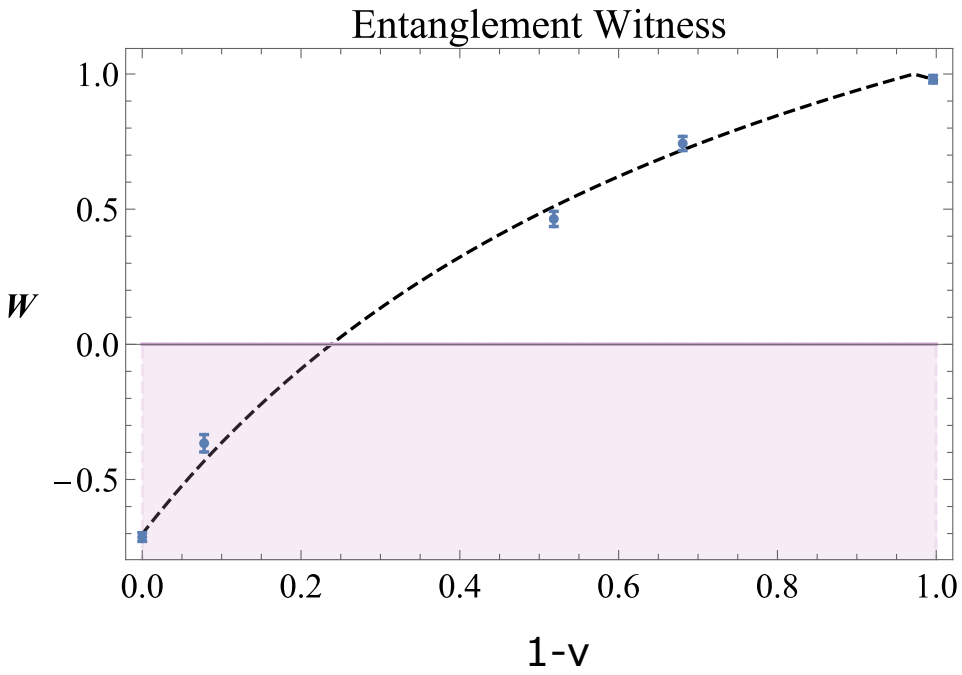

FIG. S4: **Results of QC simulator with delays between the time arrivals of the photons.** Values of the witness $\mathcal{W}$ measured as function of the degree of distinguishability $(1 - v)$ that is varied by changing the relative time delay between the photons. All error bars are due to Poissonian statistics of the measured events. The purple line indicates the value, above which the state does not violate the entanglement witness, and the shadowed area indicates the region where the witness certifies the entanglement of the state. The dashed black line represents the theoretical curve from the model of the experimental setup.